The EMBO Journal Vol.18 No.17 pp.4608–4618, 1999

Structure of the ligand-binding domain of oestrogen receptor beta in the presence of a partial agonist and a full antagonist

Ashley C.W.Pike, Andrzej M.Brzozowski, Roderick E.Hubbard[1], Tomas Bonn[2], Ann-Gerd Thorsell[2], Owe Engström[2], Jan Ljunggren[2], Jan-Åke Gustafsson[3] and Mats Carlquist[1,2]

Structural Biology Laboratory, Chemistry Department, University of York, York YO10 5DD, UK, [2]Karo Bio AB, NOVUM, S-14157 Huddinge and [3]Departments of Medical Nutrition and Biosciences, Karolinska Institute, NOVUM, S-14186 Huddinge, Sweden

[1]Corresponding authors
e-mail: rod@yorvic.york.ac.uk and mats.carlquist@karobio.se

Oestrogens exert their physiological effects through two receptor subtypes. Here we report the three-dimensional structure of the oestrogen receptor beta isoform (ERβ) ligand-binding domain (LBD) in the presence of the phyto-oestrogen genistein and the antagonist raloxifene. The overall structure of ERβ-LBD is very similar to that previously reported for ERα. Each ligand interacts with a unique set of residues within the hormone-binding cavity and induces a distinct orientation in the AF-2 helix (H12). The bulky side chain of raloxifene protrudes from the cavity and physically prevents the alignment of H12 over the bound ligand. In contrast, genistein is completely buried within the hydrophobic core of the protein and binds in a manner similar to that observed for ER's endogenous hormone, 17β-oestradiol. However, in the ERβ–genistein complex, H12 does not adopt the distinctive 'agonist' position but, instead, lies in a similar orientation to that induced by ER antagonists. Such a sub-optimal alignment of the transactivation helix is consistent with genistein's partial agonist character in ERβ and demonstrates how ER's transcriptional response to certain bound ligands is attenuated.

Keywords: activation function-2/antagonist/crystal structure/oestrogen receptor/phyto-oestrogen

Introduction

Oestrogens play a critical role in the growth, development and maintenance of a diverse range of tissues. They exert their physiological effects via the oestrogen receptor (ER), which functions as a ligand-activated transcriptional regulator (Tsai and O'Malley, 1994). Until recently, these effects were attributed to a single ER. The unexpected discovery of a second ubiquitous ER, termed ERβ (Kuiper *et al.*, 1996; Ogawa *et al.*, 1998), has added another layer of complexity to the action of oestrogens and prompted intense interest in the respective role of each isoform (Katzenellenbogen and Korach, 1997). The two ER isoforms exhibit overlapping but distinct tissue distribution patterns and differ in their ligand-binding ability and transactivational properties (Kuiper *et al.*, 1997; Barkhem *et al.*, 1998; McInerney *et al.*, 1998). Preliminary data from ER knockout studies demonstrate that each isoform has a separate biological role (Korach, 1994; Krege *et al.*, 1998).

ER is a member of a large family of nuclear receptor (NR) transcription factors with a characteristic modular structural organization with distinct domains associated with transactivation, DNA binding and hormone binding (Tsai and O'Malley, 1994). ERα and ERβ share modest overall sequence identity (47%) with little or no detectable homology between their N-terminal transactivation (AF-1) domains but well conserved DNA- and ligand-binding domains. The C-terminal ligand-binding domain (LBD) is multifunctional and, in addition to harbouring a ligand recognition site, contains regions for receptor dimerization and ligand-dependent (AF-2) transactivation (Fawell *et al.*, 1990; Danielian *et al.*, 1992). Hormone binding to ER-LBD induces a conformational change in the receptor that initiates a series of events that culminate in the activation or repression of responsive genes (Tsai and O'Malley, 1994; Beato and Sanchez-Pacheco, 1996). The precise mechanism by which ER affects gene transcription is poorly understood but, at least in the case of AF-2 activation, appears to be mediated by numerous nuclear factors that are recruited by the DNA-bound receptor (reviewed in Torchia *et al.*, 1998).

ER is an important pharmaceutical target for hormone replacement in menopausal women and for chemotherapeutic drugs against certain reproductive cancers. A wide repertoire of structurally distinct compounds bind to ER with differing degrees of affinity and potency (Anstead *et al.*, 1997; Kuiper *et al.*, 1997; Barkhem *et al.*, 1998). Some of these compounds, such as ER's natural ligand, 17β-oestradiol (E_2), act solely as receptor agonists, whereas others, typified by EM-800 and ICI 164,384, function as pure antagonists (MacGregor and Jordan, 1998). A third category, termed selective ER modulators (SERMS), have the ability to act as both agonists and antagonists depending on the cellular and promoter context as well as the ER isoform targeted (Grese *et al.*, 1997; Paech *et al.*, 1997; MacGregor and Jordan, 1998). SERMS, such as raloxifene (RAL) and tamoxifen (OHT), are used clinically in the treatment of osteoporosis and hormone-dependent breast cancer. RAL is a highly effective anti-oestrogen in the reproductive tissues but acts as a partial ER agonist in bone and also lowers blood cholesterol levels (Draper *et al.*, 1996; Gustafsson, 1998; Jordan, 1998). A variety of endocrine disrupters present in the environment also target ER. Phyto-oestrogens are a diverse group of oestrogenic compounds produced by plants primarily as bactericidal and fungicidal agents. They

represent the major natural exogenous source of oestrogenic molecules and may affect human health. The presence of such compounds in the human diet appears to be beneficial and may even confer reduced risk of hormone-dependent breast and prostate cancer, and heart disease, and alleviate symptoms associated with the menopause (Adlercreutz and Mazur, 1997). Genistein (GEN), an isoflavonoid phyto-oestrogen that is found at significant levels in soya beans and soy products, binds to both ER isoforms with moderate affinity but exhibits a preference for ERβ (Kuiper *et al.*, 1997; Barkhem *et al.*, 1998).

Previous crystallographic analyses of a number of unliganded and liganded NR-LBDs have revealed a canonical fold for the NR-LBD (Wurtz *et al.*, 1996; Moras and Gronemeyer, 1998). Eleven major helices are arranged together in an antiparallel, three-layered sandwich topology. In each case, the receptor's cognate hormone binds within a hydrophobic cavity buried within the core of the molecule. Agonist binding induces a conformational rearrangement in the LBD (Bourguet *et al.*, 1995; Renaud *et al.*, 1995) resulting in the formation of a specific binding site for the helical NR-box module of nuclear coactivators (Darimont *et al.*, 1998; Nolte *et al.*, 1998). In the case of ER, bound receptor antagonists, such as RAL, sterically prevent the correct assembly of the AF-2 region and the NR-box binding cleft (Brzozowski *et al.*, 1997; Shiau *et al.*, 1998).

We have previously described the structure of ERα-LBD in the presence of its natural ligand, E_2, and the mixed agonist/antagonist RAL (Brzozowski *et al.*, 1997). Here we present the first structural description of ERβ-LBD in complex with RAL and the β-selective partial agonist GEN. These structures, together with those already determined for ERα, provide a unique insight into the ligand-binding properties of the two ER isoforms and their response to certain ligands.

Results

Overall structure

The overall structure of the ERβ-LBD framework is identical in the two ligand complexes and similar to that observed for ERα-LBD (Brzozowski *et al.*, 1997; Shiau *et al.*, 1998; Tanenbaum *et al.*, 1998). The core of the canonical NR-LBD sandwich motif (H2–H11) is maintained with only minor differences in the length and relative orientation of the helices. A central layer of tightly packed helices, composed of H5, H6, H9 and H10, is flanked on one side by H7, H8 and H11 and on the other by H2–H4. A substantial hormone-binding cavity lies immediately below H6 and sandwiched between the outer flanking layers. The position adopted by H12 is, however, very different in the two complexes (Figure 1).

Both human (GEN complex) and rat (RAL complex) ERβ-LBD have been used in this study. These ERβs possess different size AF1 domains, but their LBD sequences are highly homologous and vary at only 20 positions between residues 254 and 504 {301–553} (Figure 2). Hereafter, the sequence numbering of human ERβ (hERβ; Ogawa *et al.*, 1998) is used for both ERβ-LBD complexes and the corresponding numbering of hERα is given in curly parentheses. The regions of high sequence variability between ERα and ERβ map to the N-terminus prior to H3 and to a stretch of 35 residues in the vicinity of H10 at the top of the LBD. This distribution is similar to that observed when comparing ERα sequences from different species alone. Only two changes, at positions 336 {384} and 373 {421}, fall within the ligand-binding cavity (Figure 2).

There are slight differences in the conformations of three regions of the structure that are induced due to changes in the crystalline environment. The short H1 observed in ERα is absent from both ERβ complexes as the first 7–8 residues at the N-terminus are disordered. In addition, the loop regions connecting H2 and H3 (residues 282–289 {329–337}) and H9 and H10 (410–428 {458–477}) exhibit different conformations in the two structures (Figure 1A and B). In the (rat) rERβ–RAL complex, the H9–H10 loop packs tightly against an adjacent molecule within the crystal lattice. This has the effect of bending the N-terminal end of H10 to one side so that it deviates by 20° relative to its position in ERα. Conversely, in the hERβ–GEN complex, where this region is not involved in intermolecular contacts, the loop connecting H9 and H10 is poorly ordered and the N-terminal end of H10 is foreshortened (Figure 1B). The only significant structural difference in the framework region of ERα and ERβ concerns the relative positioning of H5. In both ERβ structures, the N-terminal end of H5 (322–328 {370–376}) is shifted 1.5 Å away from H3 and towards H9 and H10 (Figure 1C). This has a subtle effect on the positioning of the side chains of Leu324 {372} and Val328 {376}, resulting in a slight widening of the hydrophobic groove between H3 and H5 in the region adjacent to Lys314 {362}.

In both ERβ complexes, the LBDs are packed so that the dimer axis coincides with a crystallographic dyad. The arrangement of molecules within the ERβ-LBD dimer is identical to that seen previously for ERα (Brzozowski *et al.*, 1997) and other NRs (Bourguet *et al.*, 1995). The side chains of Met403 {451}, Ala456 {505}, Met460 {509} and Leu462 {511} form a central, tightly packed hydrophobic interface at the N-terminal end of H11 that is stabilized on each side by a network of hydrogen-bonding residues. The C_α r.m.s. deviation between the non-crystallographic ERα- and crystallographic ERβ-LBD–RAL dimers is 0.97 Å (393 equivalent atoms excluding H12).

Ligand recognition

The two compounds studied here are examples of the non-steroidal class of ER ligands but they possess a diphenolic structural core that has similarities to the steroidal nucleus of E_2 (Figure 3). The ligand-binding cavity of ER is buried deep within the hydrophobic core of the LBD and surrounded by parts of H3, H6, H8, H11 and H12. Twenty-two residues, predominantly hydrophobic in character, line the cavity and interact with the bound ligands. For convenience, the different regions of the ligand-binding cavity are referred to with reference to the binding mode of the A-, B-, C- and D-rings of E_2 (Brzozowski *et al.*, 1997).

Genistein binding

GEN binds across the cavity between H3 and H11 in a manner reminiscent of that observed for E_2 (Brzozowski

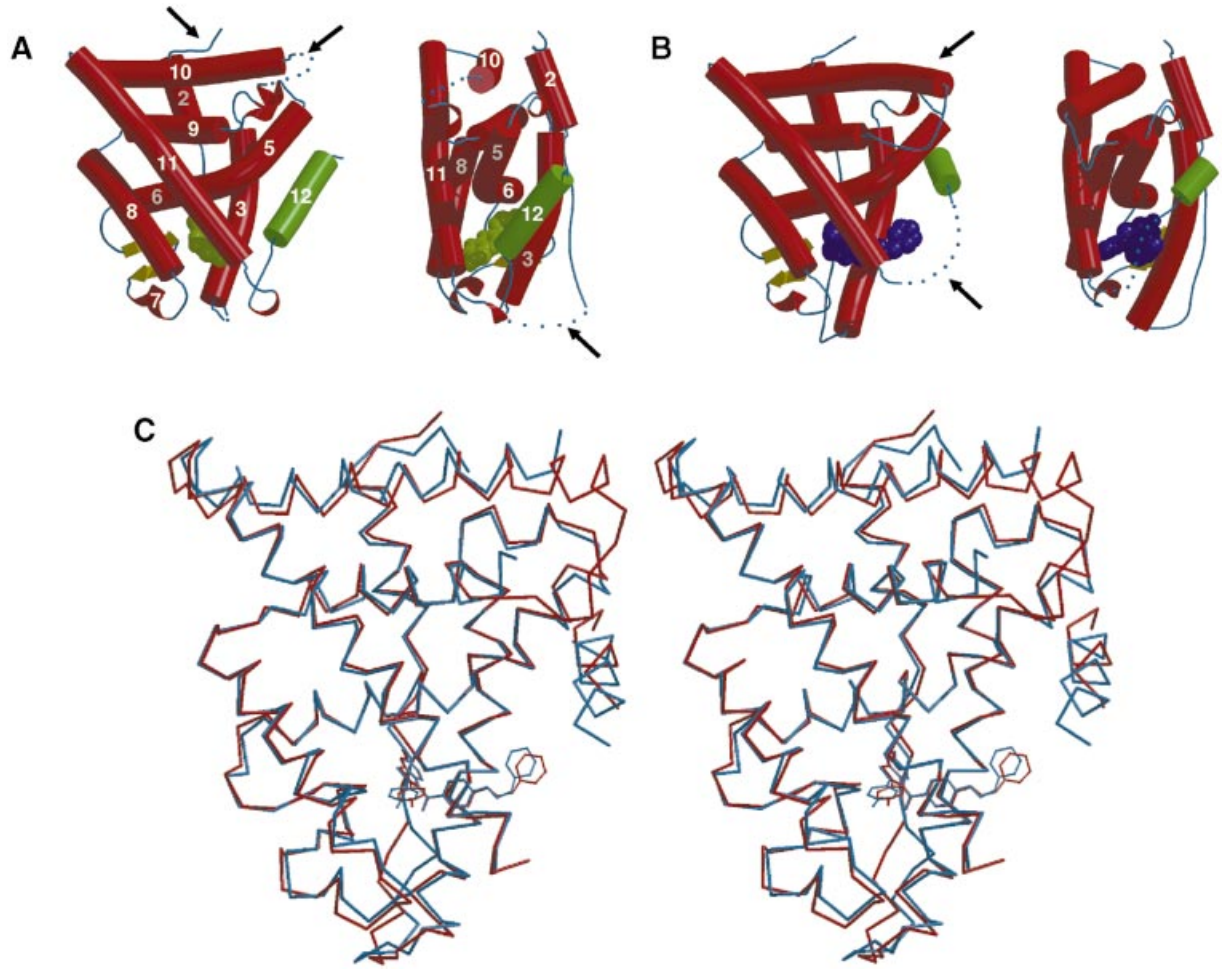

Fig. 1. Schematic representations of (**A**) the hERβ–GEN complex and (**B**) the rERβ–RAL complex. Helices are depicted as rods, 3_{10} helices as ribbons and strands as arrows. H12 is coloured green. Unmodelled regions of the structures are depicted as broken lines. Arrows indicate regions of the structure that differ between the two complexes (see text for details). (**C**) Stereoview of C_α traces of superposed coordinates of rERβ–RAL (red) and hERα–RAL (cyan; Brzozowski *et al.*, 1997) LBD complexes.

et al., 1997; Tanenbaum *et al.*, 1998). The phenolic ring mimics the A-ring of E_2 and is clamped in the narrow cleft between H3, H6 and the β-hairpin. The phenolic hydroxyl (O14) interacts with the side chains of Glu305 {353} and Arg346 {394} and a buried water molecule (Figure 4A and B). The flavone portion of GEN occupies a position similar to that adopted by the C- and D-rings of E_2 and is orientated so that the O2 hydroxyl (see Figure 3A for atom numbering scheme) makes a hydrogen bond with His475 {524} at the distal end of the cavity (Figure 4A and B). The imidazole side chain of His475 {524} is held in the correct position to act as a hydrogen bond acceptor by a second hydrogen bond between its $N_{\varepsilon 2}$ group and the main chain carbonyl of Glu371 {419}. The hydrogen-bonding potential of the remaining polar moieties of the flavone ring is not satisfied by interaction with the protein. Instead, the ring oxygen (O9) is directed towards the unoccupied pocket on the β-face of the cavity and the ring hydroxyl (O4) and keto group (O6) point toward the α-face pocket (Figure 4B). The O4 hydroxyl, which occupies the same position within the cavity as 15α substituents of E_2, presumably participates in an intramolecular hydrogen-bonding interaction with the O6 keto group. Figure 4C illustrates the similarity in the binding modes of GEN and E_2. The longer hydroxyl–hydroxyl length of GEN (12.1 Å), compared with that of E_2 (10.8 Å), is accommodated at the D-ring end of the cavity by a slight shift of H11 combined with the outward movement of His475 {524}.

Despite being entirely engulfed by the protein, direct van der Waals contacts between GEN and the residues lining the cavity are concentrated around the extremities of the ligand (Figure 4A). The binding cavity in the hERβ–GEN complex has a volume of 390 $Å^3$ of which 236 $Å^3$ is occupied by the ligand. This overall cavity size is slightly smaller than that of ERα–E_2, which has a probe-occupied volume of 490 $Å^3$, and this reduction is due primarily to the replacement of the leucine at position 336 {384} in ERα by a bulkier methionine in ERβ. This conservative substitution reduces the size of the unoccupied pocket that lies above the ligand. It is noteworthy that Met336 is the only residue within the ligand-binding cavity that exhibits static disorder and has been modelled in a major (70%) and minor (30%) conformation. In addition to this sequence change, the more planar profile of GEN compared with E_2 allows the residues that line the cavity to pack slightly more tightly around the ligand in ERβ.

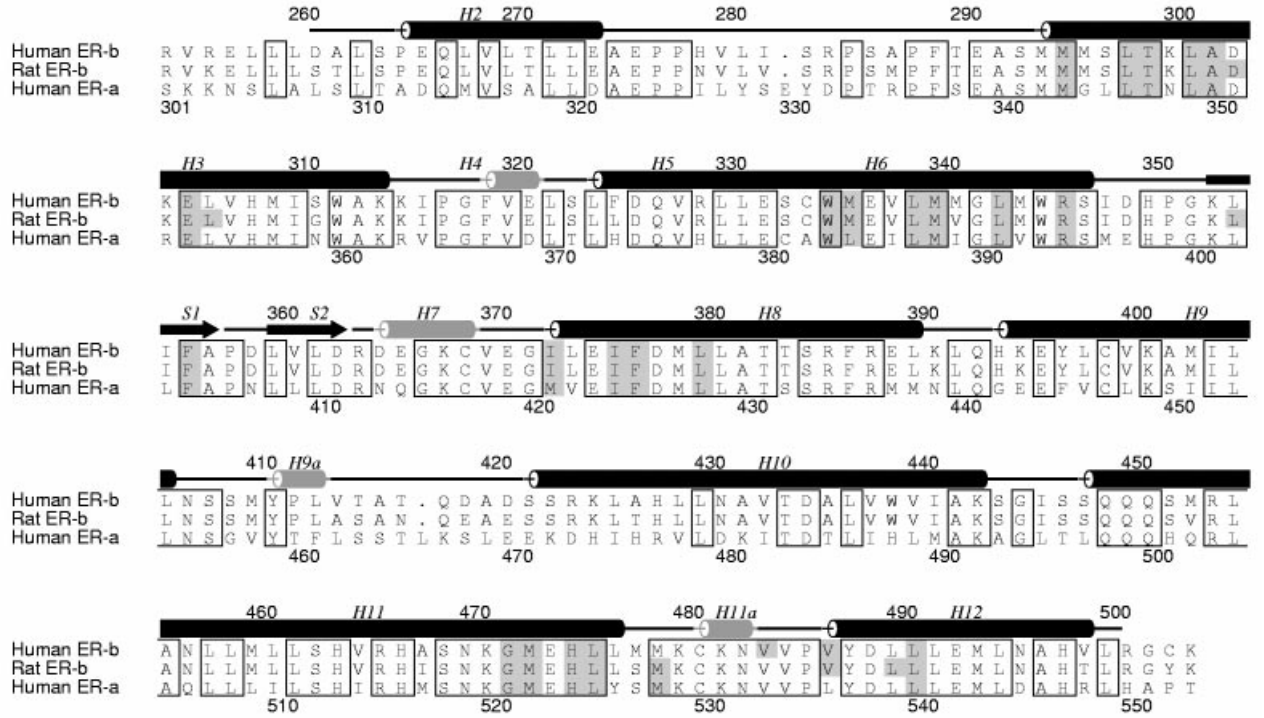

Fig. 2. Alignment of the human and rat ERβ-LBD amino acid sequences against human ERα-LBD. The secondary structure of the hERβ-LBD–GEN complex is shown schematically along with nomenclature. Helices are represented by solid cylinders, 3_{10} helices as grey shaded cylinders and β-strands as arrows. The numbering of human ERβ-LBD is shown along the top of the alignment with the corresponding numbering of human ERα-LBD at the bottom. Regions of identity are boxed and residues that line the hormone-binding cavity and/or interact with bound ligand (GEN, RAL or E_2) are shaded in light grey. The figure was produced using the program ALSCRIPT (Barton, 1993).

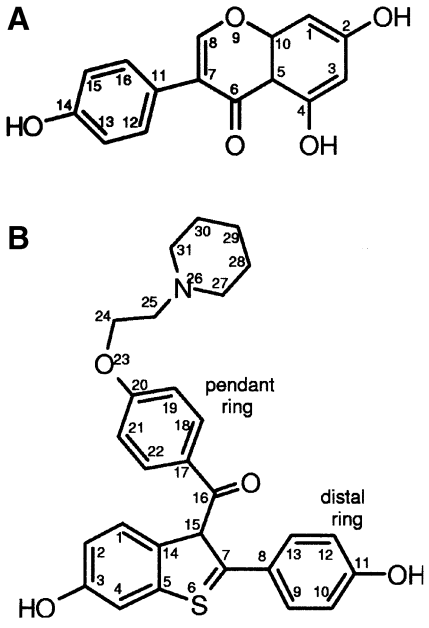

Fig. 3. Chemical structures of (**A**) GEN and (**B**) RAL showing the atom numbering scheme and ring nomenclature used in the text.

Raloxifene binding

RAL is accommodated within the binding cavity in the same manner as that observed in the ERα complex (Brzozowski *et al.*, 1997). The phenolic hydroxyl of the benzothiophene interacts with Glu305 {353}, Arg346 {394} and a structurally conserved water molecule (Figure 5A). The hydroxyl of the distal ring hydrogen-bonds with His475 {524}. However, the rigid nature of the aroylbenzothiophene core in combination with the architecture in the A-ring pocket and the location of the channel exiting the cavity results in a different mode of binding compared with GEN. The distal end of RAL is thrust deeper into the D-ring end of the cavity towards H8. The orientation of each ligand, relative to their major hydroxyl–hydroxyl axis, differs by ~20° so that the respective hydroxyls that interact with His475 {524} are separated by 3.9 Å (Figure 5B).

The large basic side chain of RAL binds in a narrow channel that extends outward from the centre of the cavity. This channel is present in the hERβ–GEN complex but it is plugged by Val487 {536}. The end of the side chain is anchored to H3 by a hydrogen bond between the carboxylate group of Asp303 {351} and the piperidine ring nitrogen. The weak nature of this interaction, compared with that observed in the corresponding ERα complex, may be related to the low pH at which the rERβ–RAL crystals were obtained. Van der Waals contacts between RAL and residues that line the cavity are concentrated around the hydroxyl recognition sites and along the length of the side chain moiety (Figure 5A). The rERβ-LBD undergoes a series of concerted changes, in both secondary and tertiary structure, on binding of RAL. The residues that define the 'neck' of the channel (Thr299 {347}, Ala302 {350} and Trp335 {383}) move outward to accommodate the pendant ring of the side chain. For the most part, this is achieved by the movement of the N-terminal half of H3 (293–304 {341–352}), by between 0.8 and 1.4 Å, away from the ligand-binding cavity. In an associated movement on the opposite side of the cavity,

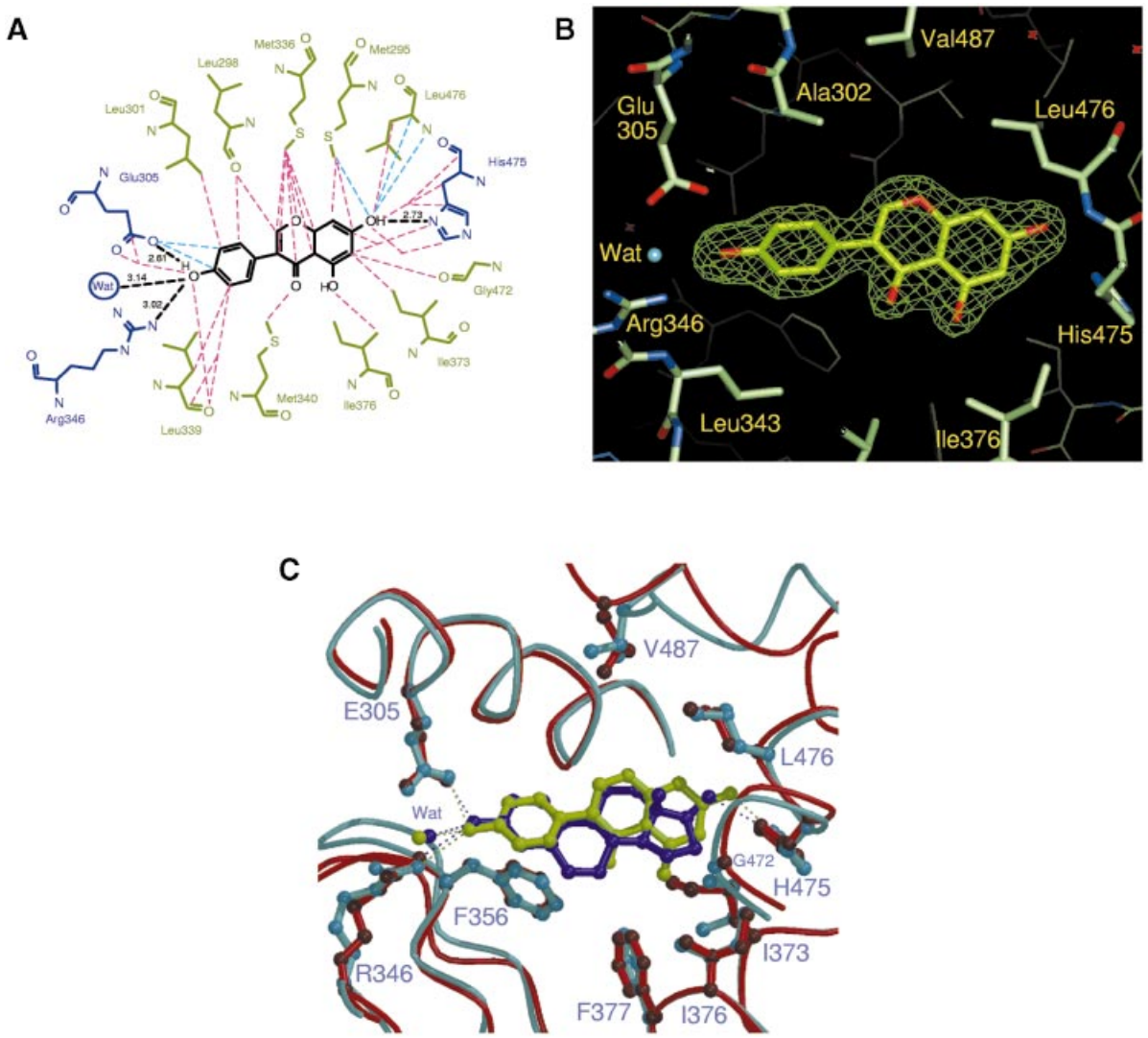

Fig. 4. (**A**) Schematic representation showing GEN and its interactions with the hERβ-LBD. Residues within the binding cavity that make at least one contact within 3.8 Å of each ligand are shown. Residues making hydrogen bonds are coloured blue and those making van der Waals contact are coloured green. Interactions between the protein and ligands are depicted as broken lines (hydrogen bonds and distances in black; $d \leqslant 3.3$ Å in cyan; 3.3 Å$<d\leqslant$3.8 Å in pink). (**B**) Omit $|F_{obs}| - |F_{calc}|$ electron density map contoured at 3σ for the ligand-binding cavity in the hERβ–GEN complex. The map was phased using a model in which GEN had been excluded. Atoms are coloured according to type [carbon: pale green (protein), dark green (GEN); oxygen: red; nitrogen: blue]. (**C**) Comparison of ligand-binding mode of GEN (protein, light blue; ligand, green) in hERβ-LBD and E_2 (protein, red; ligand, purple) in hERα-LBD (PDB code: 1ERE) within the cavity. The ligands are viewed looking down from the β-face of the cavity and only those side chains that interact with the bound ligand or exhibit different orientations are shown. Hydrogen bonds are depicted as broken lines.

H7 and the H7–H8 loop (residues 367–373 {415–421}) are shifted in towards the bound RAL, presumably to compensate for the outward motion of H3 (Figure 5B). A similar, but more dramatic, movement of the H7–H8 loop occurs in the ERα–OHT complex (Shiau *et al.*, 1998).

Cavity plasticity

While the residues within the cavity exhibit different spatial positions in the two ERβ complexes due to shifts in cavity scaffold, most of the side chains that line the cavity adopt identical rotamer conformations. There are, however, several notable exceptions. The different binding modes of each ligand at the D-ring end of the cavity affect the orientation of Ile373 {421}, His475 {524} and Leu476 {525}. The imidazole ring of His475 {524} twists in response to the different distal hydroxyl positions of the two ligands in order to maintain an optimal position for hydrogen bonding. Leu476 {525}, situated on the β-face of the cavity, adjusts its position to compensate for each ligand's different binding mode at the D-ring end of the cavity. When GEN is bound, the side chain is flipped up away from the flavone ring but, in the presence of RAL, it is flipped down toward the distal ring. Similarly, Ile373 {421}, located on the α-face of the cavity, rotates in toward the cavity in the RAL complex to pack against the distal phenolic ring (Figure 5B).

At present, RAL represents the only ligand for which structures are available with both ERα- and ERβ-LBD, and their comparison provides clues as to the differences in the plasticity of the cavity of the two isoforms. The r.m.s deviation for all ligand atoms, after superposition of the hERα–RAL and rERβ–RAL complexes, is 0.52 Å.

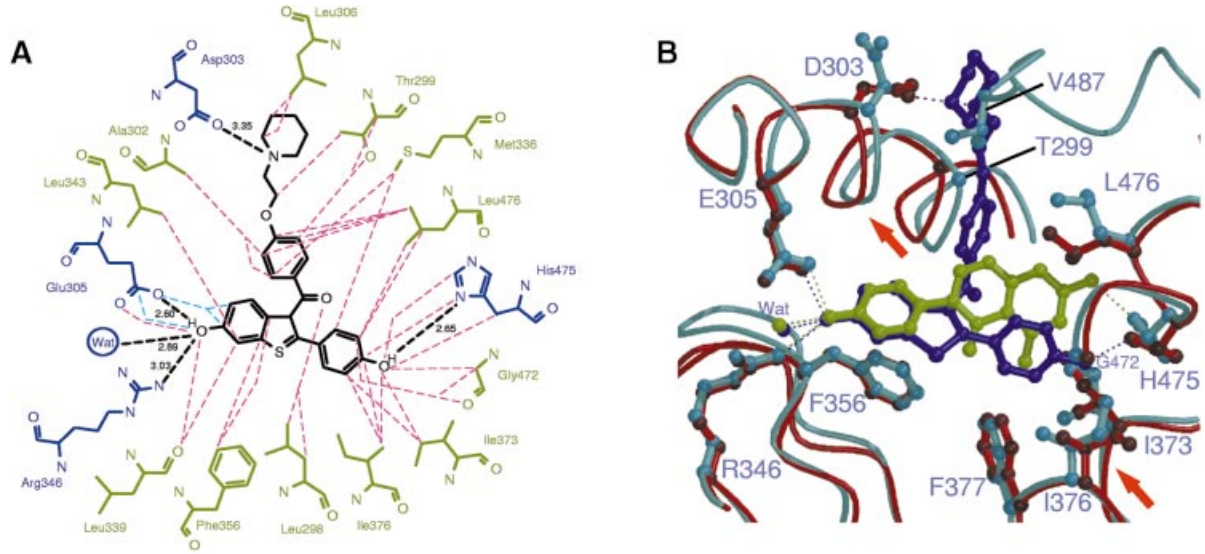

Fig. 5. (**A**) Schematic representation showing the interactions between RAL and rERβ-LBD. Distance cut-offs and colouring used are as in Figure 4A. (**B**) Comparison of the ligand-binding mode of GEN (protein, light blue; ligand, green) and RAL (protein, red; ligand, purple) within the rERβ-LBD binding cavity. Solid arrows highlight concerted shifts in the framework of the cavity that accompany the binding of RAL. The binding cavity is viewed in the same orientation as in Figure 4C.

The benzothiophene and pendant rings occupy identical relative positions. However, in ERβ, the distal phenolic ring of the ligand is thrust less deeply into the D-ring end of the cavity. The difference in the position of the distal hydroxyl in the two isoforms is 1.4 Å. As a consequence, the imidazole ring of His475 {524} maintains its positioning interaction with the backbone carbonyl of Glu371 {419} in the ERβ complex. In addition, the end of the basic side chain adopts a more extended conformation in rERβ–RAL, resulting in a 0.9–1.5 Å outward shift of the piperidine ring. This alteration in the basic side chain is presumably imposed by the different conformation of the H11–H12 loop and positioning of H12 in the rERβ–RAL complex. The residues lining the core of the cavity pack around the ligand in a similar manner, with only Phe377 {425} adopting a different orientation. In rERβ–RAL, the benzyl group of this residue is tucked up under the distal phenolic ring of the RAL core but does not make direct van der Waals contact with ligand. In contrast, in the hERα–RAL complex, the side chain is flipped away from the ligand resulting in the enlargement of the unoccupied pocket on the α-face of the cavity. This difference is probably due to the amino acid substitution of an isoleucine (ERβ) for a methionine in ERα at position 373 {421}. In ERα, RAL binding induces the repositioning of the methionine side chain, towards Phe377 {425}, and displaces the ring. In ERβ, these positional adjustments can be accommodated without displacement of Phe377 due to the smaller size of the isoleucine side chain.

There are now sufficient structures of ERs in different space groups and at different pHs to permit a meaningful analysis of the relative mobilities of the ligand-binding cavity. Analysis of the temperature factors of the residues that line the ligand-binding site in the two RAL complexes indicates a similar degree of mobility within the cavity of ERα and ERβ. The A-, B- and C-ring regions exhibit very similar mobilities, but the residues lining the D-ring region of rERβ–RAL have *B*-values that are typically 1.5 times higher than those of the other sites. A similar pattern of cavity subsite mobility (A≈B≈C<D) is observed in ERα irrespective of the bound ligand (A.C.W.Pike, unpublished results), but the increase at the distal end of the pocket is less pronounced. The higher observed D-ring mobility in the presence of RAL presumably reflects the greater degree of distortion imparted by the binding mode of the distal phenolic ring of the aroylbenzothiophene core.

Helix 12 positioning

Both ligands induce a conformation of the AF-2 region that is distinct from that observed in the presence of pure agonists (Figure 6).

The binding of RAL is accompanied by a major reorganization in the tertiary structure of ERβ-LBD. In particular, the bulky side chain of RAL physically prevents H12 from adopting its characteristic position over the ligand-binding cavity. Instead, H12 lies in a shallow groove formed between H3, H4 and H5 (Figure 6A). As in the hERα–RAL complex, the loop connecting H11 and H12 (Met479–Pro486 {529–535}) is invisible in the electron density maps. H12 itself is highly disordered and the resultant modelled helix has high *B*-values. In addition, only those side chains on its inner face (Leu491 and Leu495), that pack against H5, can be resolved. Nonetheless, the position occupied by H12 is similar to that observed for this region in the hERα–RAL complex except that it is shifted along the hydrophobic groove by between 1.9 and 3.2 Å. In the rERβ–RAL complex, Leu491 {540} packs against the side chains of Val328 {376} and Leu331 {379}. Leu495 {544} makes van der Waals contact with residues in H3 (Ile310 {358}), H4 (Phe319 {367}) and H5 (Leu324 {372} and Val328 {376}). The side chain of Lys314 {362} makes hydrogen bonds with the main chain carbonyl groups of Met494 {543} and Leu495 {544} and effectively caps the C-terminal end of H12 (Figure 6A).

The groove in which H12 lies in the RAL complex also represents the binding site for the helical NR-box module of nuclear coactivators (Feng *et al.*, 1998). In fact, the spatial positions of Leu491 {540} and Leu495 {544} coincide with the first and third NR-box leucine residues

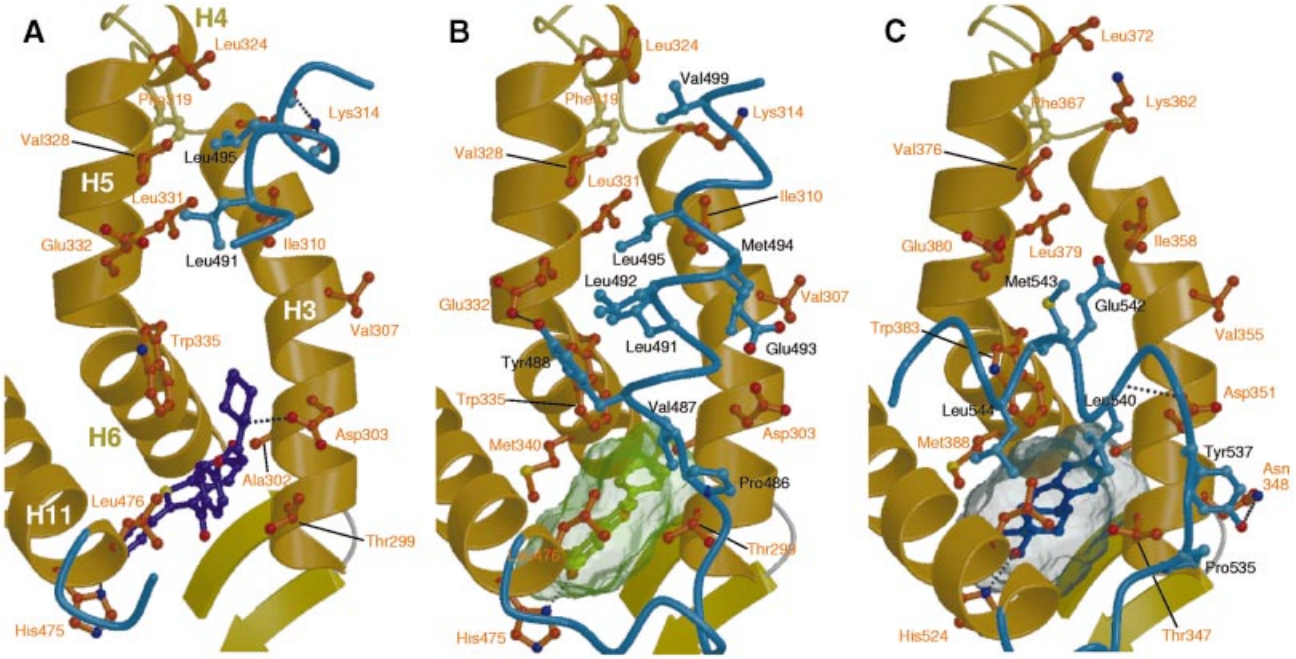

Fig. 6. Positioning of H12 in (**A**) RAL and (**B**) GEN complexes with ERβ-LBD and (**C**) the ERα-LBD–E_2 complex. H12 and the H11–H12 loop (blue) are shown along with parts of H3, H5, H6, H11 (gold) and the S1–S2 β-hairpin (yellow). Residues that interact with the three conformations of H12 are shown and labelled in orange [hERβ numbering is used for (A) and (B), and hERα numbering is used for (C)]. The interacting residues in the H11–H12 loop and H12 are labelled in black. The extent of the enclosed cavity in GEN and E_2 complexes is represented by the transparent surfaces. Hydrogen bonds are depicted by broken lines.

of the GRIP1 peptide (Shiau *et al.*, 1998). This reinforces the previous observation that H12 in ER antagonized by RAL and OHT mimics the interaction of coactivator peptides (Brzozowski *et al.*, 1997; Shiau *et al.*, 1998). The anchoring of the end of the antagonist side chain by Asp303 {351} serves to direct H12 into the coactivator-binding site. The importance of this tethering interaction is given further weight by the discovery of a drug-resistant breast cancer cell line in which Asp303 {351} is mutated to tyrosine and the antagonistic effects of RAL are reduced considerably (Jordan, 1998). Together, these observations provide a structural rationale for the known interdependence of RAL antagonism and the length and positioning of the basic nitrogen within the side chain (Grese *et al.*, 1997).

In the hERβ–GEN complex, H12 also lies between H3 and H5. There are, however, fundamental differences in the length, positioning and interactions made by H12 compared with the 'antagonist' orientation induced by RAL. H12 is longer, comprising four turns of α-helix (residues 487–499 {536–548}), and is well defined in the electron density. At the end of H11 (Leu477 {526}), the main chain turns through 90° running along H3, past the entrance to the ligand-binding cavity, and continues, as H12, in a direction parallel to H5 (Figure 6B). Val487 {536} rests in the gap at the entrance of the ligand-binding cavity between H3, H6 and H11, and contacts Thr299 {347}, Ala302 {350}, Leu306 {354} and Trp335 {383}. The insertion of Val487 at the entrance of the cavity forces H12 to adopt a different orientation along the hydrophobic groove compared with that observed in the rERβ–RAL complex. There is a 25° difference in helix orientation between the two complexes. Rather than running along the hydrophobic groove, H12 projects away from the body of the protein in the GEN structure. The N-terminal end packs close to the protein, with Leu491 {540} making van der Waals contact with Trp335 {383}. Met494 {543} lies on the edge of the groove against H3 and contacts Leu306 {354}, Val307 {355}, Ile310 {358} and Asp303 {351}. The position of Leu495 coincides with that of Leu491 in the RAL complex and it makes similar contacts. In addition to these hydrophobic contacts, this unique disposition of H12 is stabilized by a specific hydrogen bond between the phenolic hydroxyl of Tyr488 {537} and the carboxylate side chain of Glu332 {380} in H5 (Figure 6B).

Discussion

In this study, we report the first description of the structure of ERβ's LBD in the presence of a partial agonist and full antagonist. These complexes shed light on the structural basis for each ligand's differential pharmacological effects through ERβ and provide some clues as to the determinants of isoform-selective ligand binding. As expected from the high sequence identity between the LBDs of the two isoforms, their tertiary and quaternary structure are very similar. While both ER isoforms readily form homodimers, their overlapping cell and tissue distribution raises the possibility of heterodimerization. Formation of mixed dimers has been demonstrated both *in vitro* and *in vivo* (Ogawa *et al.*, 1998), but the physiological role of the heterodimer is unclear. Nonetheless, the exclusive substitution of a methionine at positions 403 {451} and 460 {509} within the hydrophobic patch of H11 of ERβ has no impact on the dimer interface and suggests that the arrangement of molecules in an α/β heterodimer will be the same.

α/β ligand selectivity

The size and shape of the ER ligand-binding cavity, combined with the plasticity of its component elements,

allows ER to embrace a range of ligands containing a variety of structural motifs (Anstead *et al.*, 1997; Brzozowski *et al.*, 1997; Shiau *et al.*, 1998). The generous size of the binding cavity coupled with the variety of known ligand-binding modes (Brzozowski *et al.*, 1997; Shiau *et al.*, 1998) suggests that receptor selectivity in ER can be generated through a number of different interactions. This contrasts with the situation in other NRs, such as thyroid receptor (TR) and the retinoic acid receptor (RAR), where the cavity shape is well matched to that of the cognate hormone and the stability of the complex is dependent on a large number of hydrophobic interactions. For example, in RAR, the inherent flexibility of the receptor ligands allows them to adapt to the shape of the binding cavity, and isoform selectivity can be determined by a few key interactions (Klaholz *et al.*, 1998).

In the case of ERα and ERβ, the relatively invariant tertiary architecture of the binding cavity explains why the majority of compounds bind to each isoform with similar affinities (Kuiper *et al.*, 1997). The two conservative amino acid changes within the binding cavity have a direct impact on its overall volume and may also be responsible for the distinct ligand-binding preferences reported for ERβ (Barkhem *et al.*, 1998). GEN binds preferentially to ERβ with a 30-fold higher affinity (Kuiper *et al.*, 1997; Barkhem *et al.*, 1998). The two cavity-lining residues that differ between ERα and ERβ are obvious candidates for this selective effect. As mentioned above, the leucine present at position 336 {384} in H6 of ERα is replaced by a methionine in ERβ. This residue lies above the ligand and delineates part of the pre-formed pocket on the β-face of the cavity. In the hERβ–GEN complex, the side chain of this residue makes direct van der Waals contact with part of the flavone ring. While methionine is generally considered to be hydrophobic in nature, the sulfur has a weak polar character and participates in hydrogen-bonding interactions in proteins (Stickle *et al.*, 1992). The sulfur group of the methionine adopts two distinct, but unequally occupied alternative positions in the hERβ–GEN complex. In one of these positions, the sulfur is 4.6 Å from the keto moiety of the flavone ring but this interaction is unlikely to provide sufficient stabilization due to the large inter-atomic distance. Furthermore, the static disorder exhibited by this atom indicates that such an interaction is unlikely to be responsible for GEN's higher affinity for ERβ.

The second substitution within the cavity replaces a methionine at position 373 {421} at the start of H8 (ERα) by an isoleucine (ERβ). This residue lies on the α-face of the cavity immediately below the D-ring of E_2 and is sandwiched between His475 {524} and Phe377 {425}. Polar substitutions are poorly tolerated at the D-ring end of the cavity in ERα (Anstead *et al.*, 1997) and, in particular, at the 15α position where the O4 hydroxyl of GEN's flavone ring lies. Perhaps the migration of the weakly polar methionine from the α- to the β-face of the cavity enables ERβ to accommodate more polar substituents at the distal end of the cavity. In summary, the distinct ligand-binding preference of GEN for ERβ is difficult to reconcile convincingly on the basis of these sequence differences alone.

Determinants of H12 alignment

The reasons for the misalignment of H12 in the RAL complex are clear; the basic side chain protrudes from the cavity and physically prevents its positioning over the hormone-binding site. In fact, the piperidine ring of the basic side chain occupies the same spatial position as Val487 {536} in the GEN complex. GEN, on the other hand, has a similar molecular volume (236 $Å^3$) to that of E_2 (250 $Å^3$) and binds in an analogous fashion, yet in the hERβ–GEN complex, H12 has a preference for binding along the NR-box cleft rather than over the cavity. What then determines the positioning of H12 in the hERβ–GEN complex? The amino acid sequence in the vicinity of the H11–H12 loop and H12 is highly conserved in both ER isoforms and differs at only two positions (Figure 2). This suggests that the differences in the helix positioning in the presence of these ligands is not due to any inherent difference in flexibility of this region between the two isoforms.

The primary determinant of H12 positioning appears to be the burial of its hydrophobic face against the protein and, in so doing, sealing the ligand within the binding cavity. The positions of H12 in the presence of pure agonist, such as E_2 and diethylstilbestrol (DES) (Brzozowski *et al.*, 1997; Shiau *et al.*, 1998), and that seen here in the hERβ–GEN complex both fulfil this objective. In the archetypal 'agonist' orientation, typified by the ERα–E_2 complex, the N-terminal end of H12 appears to be stabilized by two hydrophilic interactions. The helix is capped by Asp303 {351}, which interacts with the main chain amide of Leu491 {540}. In addition, Tyr398 {537} makes a hydrogen bond with Asn300 {348}. These two interactions effectively anchor the N-terminal end of H12 and position it so that Leu491 {540} can seal the ligand-binding cavity (Figure 6C). In other NRs, the 'agonist' orientation of H12 is stabilized by similar N-capping interactions and, in the case of TR and RARγ, by an additional interaction between the C-terminal end of H12 and a lysine in H5 (Renaud *et al.*, 1995; Wagner *et al.*, 1995).

Functional analyses demonstrate that ERβ is easier to antagonize than ERα (S.Nilsson, personal communication). One explanation for this observation is that the 'agonist' orientation of H12 in ERβ is more unstable than in ERα. The asparagine present at position 300 {348} in ERα, which interacts with Tyr398 {537}, is replaced by a lysine in ERβ. Consequently, the 'agonist' orientation of H12 may be less favoured in ERβ due to loss of the hydrogen-bonding interaction made by this residue to Tyr398. The slight widening at the distal end of the hydrophobic groove in ERβ compared with ERα (see above) is unlikely to be responsible for the different positioning of H12 in the GEN complex. Figure 6 clearly highlights the conformational adaptability of the H11–H12 region of ER-LBD. Despite the radically different positions adopted by H12 in the various ligand complexes, several common structural features are maintained. For example, Val487 (ERβ) and Leu540 (ERα), two residues which are not equivalent in terms of sequence (Figure 2), play an identical structural role by sealing ligand within the binding cavity of the hERβ–GEN and hERα–E_2 complexes (Figure 4C). Nevertheless, the origin of GEN's 'destabilizing' influence on H12 remains unclear, and further structural studies with full ERβ agonists are

Table I. Statistics for crystallographic structure determination

	hERβ–GEN	rERβ–RAL
Data collection details		
Data collection site	ID14-4, ESRF	X11, DESY
Wavelength (Å)	0.93	0.9096
Space group	$P6_122$	$P4_122$
Unit cell dimensions (Å)	$a = b = 63.12$, $c = 250.23$ $\gamma = 120°$	$a = b = 67.55$, $c = 148.2$
Processing statistics		
Resolution range (Å)	60–1.8	25–2.25
Observations	358 818	97 187
Unique reflections	28 523	16 904
Completeness (%)	99.7	99.0
R_{merge}[a]	4.9	7.7
Outer resolution shell		
Resolution range (Å)	1.83–1.80	2.29–2.25
Unique reflections	1370	813
Completeness (%)	100	98.7
R_{merge}[a]	43.3	46.7
Refinement statistics		
Resolution range (Å)	55–1.8	25–2.25
Reflections used (R_{free} set)	27 019 (1441)	15 179 (1691)
R_{cryst} (R_{free})[b]	21.9 (25.5)	20.4 (26.3)
Protein/ligand atoms	1834/20	1807/34
Water molecules	139	128
R.m.s. bonds/angles (Å)[c]	0.013/0.031	0.014/0.038
R.m.s. backbone ΔB (Å^2)[d]	2.3	2.2
Mean *B*-factor (Å)[e]	41/40/43/32/46	47/49/46/48/43
%A,B,L (a,b,l,p)[f]	95.7 (4.3)	95.1 (4.4)

[a]$R_{merge} = 100\times\Sigma|I - <I>|/\Sigma<I>$.
[b]$R_{cryst} = \Sigma|F_{obs} - F_{calc}|/\Sigma F_{obs}$; R_{free} is as R_{cryst} but calculated over either 5% (GEN) or 10% (RAL) of data that were excluded from the refinement process.
[c]Root mean square deviation in bond length and angle distances from Engh and Huber ideal values.
[d]Root mean square deviation between *B*-factors for bonded main chain atoms.
[e]Mean temperature factor for whole molecule, main chain, side chain, ligand and water atoms, respectively.
[f]Percentage of residues located in most favoured (additional) regions of the Ramachandran plot as determined by PROCHECK (Laskowski *et al.*, 1993).

required to understand fully the subtle inter-relationship between ligand binding and H12 orientation.

Implications for agonism and antagonism

Partial agonist activity of SERMs, such as RAL and OHT, through ERα is thought to be dependent on the N-terminal AF-1 transactivation domain rather than on AF-2 (MacGregor and Jordan, 1998). However, the AF-1 domain of ERβ is devoid of this functionality and SERMs act as pure antagonists via this receptor isoform when bound to EREs (Barkhem *et al.*, 1998; McInerney *et al.*, 1998). The partial agonism exhibited by GEN on ERβ (Barkhem *et al.*, 1998) must therefore arise through a different effect. One clue is the sub-optimal positioning of H12 in the hERβ–GEN complex.

ERs, and other nuclear receptors, recruit a variety of nuclear coactivators for optimal efficacy (Torchia *et al.*, 1998). The recruitment surface is a shallow hydrophobic groove formed between H3, H5, H6 and H12 (Feng *et al.*, 1998). In the complexes of ERα with the full agonists E_2 (Brzozowski *et al.*, 1997) and DES (Shiau *et al.*, 1998), H12 is aligned over the ligand-binding cavity so that the side chain of Leu491 {540} seals the entrance to the cavity (Figure 6C). In this orientation, the side chain of Glu493 {542} is positioned ideally to interact with the N-terminal end of the helical NR-box motifs of coactivators (Darimont *et al.*, 1998; Nolte *et al.*, 1998; Shiau *et al.*, 1998). The observation that AF-2 antagonists, such as RAL, prevent the correct alignment of H12 has provided a structural model for their effects (Brzozowski *et al.*, 1997).

The observation that the partial agonist, GEN, elicits an orientation of H12 similar to ER antagonists is intriguing. The position adopted by H12 in the presence of GEN in hERβ is not sequence dependent or a crystal packing effect, as it is also observed in a tetragonal crystal form of rERβ in complex with the same ligand (A.C.W.Pike, unpublished results). H12 has been observed to interact with the NR-box binding cleft in the structures of unliganded RXRα (Bourguet *et al.*, 1995), PPARγ (Nolte *et al.*, 1998) and Cys530-cross-linked ERα (Tanenbaum *et al.*, 1998). However, in all these cases, H12 interacts with the binding cleft of a neighbouring molecule within the crystal lattice. The hERβ–GEN complex therefore represents the first time that this orientation of H12 has been observed in the presence of ligand and suggests that occupation of the binding cleft may serve a physiological purpose. Interestingly, the conformation of H12 in the GEN complex only partially mimics that of the NR-box module. In fact, the position adopted by H12 is shifted some 4–5 Å from the position adopted by short peptides derived from the nuclear interaction domains of coactivators. The observation that H12 perfectly mimics the interactions made by NR-box peptides in ER antagonist complexes, such as that described here with RAL, has led to the suggestion that H12 may act in an autoinhibitory manner (Shiau *et al.*, 1998). Rather than an autoinhibitory response, such occupation of the cleft by H12 is more

likely to represent a mechanism through which the receptor can attenuate the effects of certain ligands. In the case of GEN, which only acts as a partial agonist through ERβ (Barkhem *et al.*, 1998), H12's preferential occupation of the NR-box binding cleft sets up a direct competition for this site with ER coactivators. Consequently, potential coactivators must therefore displace H12 into an 'agonist-like' conformation prior to binding.

Materials and methods

Protein expression, purification and crystallization

Rat and human ERβ-LBD (residues 255–509; hERβ numbering) were overexpressed in *Escherichia coli* GI 724 cells using the pLEX expression system (Invitrogen). A short FLAG™ sequence (MDYKDDDDK) was engineered prior to the N-terminus of the ERβ-LBD to facilitate antibody-mediated identification. Fermentation was carried out in fed-batch culture (defined glucose/salt medium, 30°C) and expression of the recombinant protein was induced by the addition of tryptophan (0.25 g/l). After a 3 h induction, cells were harvested by centrifugation and frozen. Thawed cells were disrupted in a bead mill in lysis buffer [100 mM Tris pH 8.1, 300 mM KCl, 10% glycerol, 5 mM EDTA, 0.1 mM phenylmethylsulfonyl fluoride (PMSF), 4 mM dithiothreitol (DTT)] and the bacterial lysate was centrifuged to pellet the cell debris. The supernatant was applied to an oestradiol–Sepharose fast flow column (Greene *et al.*, 1980) and washed with 300 mM KCl, 2 mM EDTA and 2 mM DTT in 20 mM Tris pH 8.1. Bound protein was carboxymethylated *in situ* overnight with 15 mM iodoacetic acid. After carboxymethylation, the column was washed with 100 mM KCl in 20 mM Tris pH 8.1. For the GEN complex, hERβ-LBD was eluted by including 50 μM ligand in the washing buffer. In the case of RAL, the column was washed with 250 mM NaSCN in 20 mM Tris pH 8.1 and the protein was eluted by addition of 50 μM ligand. Pooled fractions of each carboxymethylated ERβ-LBD complex were concentrated and purified further by preparative PAGE (Bio-Rad 491) using the Ornstein/Davies buffer system as per the manufacturer's instructions. Fractions were analysed by native PAGE and fractions showing a single protein band were pooled, concentrated and used for crystallization. The hERβ–GEN and rERβ–RAL complexes were crystallized using the vapour diffusion technique at 18°C. For the RAL complex, the reservoir solution contained 7.5% (w/v) PEG 4000, 0.1 M ammonium acetate, 3% (v/v) dimethylformamide in 25 mM sodium acetate pH 4.8. Drops were composed of a 2:1 ratio of protein (7–11 mg/ml) and reservoir solution. Tetragonal bipyramids, with unit cell dimensions of $a = b = 67.55$ Å $c = 148.2$ Å and containing one LBD molecule per asymmetric unit, appeared within 1–2 weeks. For the GEN complex, drops were composed of equal volumes of protein (8 mg/ml) and reservoir solution [6–9% (w/v) PEG 6000, 1.6–2.1 M NaCl in 0.1 M Tris pH 8.1]. The resultant hexagonal rods belong to space group $P6_122$ and have unit cell dimensions of $a = b = 63.12$ Å $c = 250.23$ Å with one LBD molecule per asymmetric unit.

Data collection

Initial data sets to resolutions of 2.5 Å (RAL complex) and 2.3 Å (GEN complex) were collected at station 9.5 (SRS, CLRC Daresbury, UK) and station W32 (LURE, Orsay, France), respectively. Subsequently, diffraction data for the rERβ–RAL complex were collected to 2.25 Å resolution on station X11 at DESY (EMBL, Hamburg). Data frames, corresponding to oscillations of 1.4°, were recorded using an 18 cm MAR Research image plate placed at 190 mm from the crystal. Data for the hERβ–GEN complex were collected to 1.8 Å resolution on station ID14-4 at the ESRF (Grenoble, France). Data were recorded in two sweeps using an ADSC Quantum4 CCD detector placed at 280 mm (55–3 Å) and 160 mm (1.8 Å) from the crystal, respectively, using 1° oscillations. In both cases, the crystals were cryoprotected with 25% 2-methyl-2,4-pentanediol prior to freezing at 100 K. All data were integrated and reduced using DENZO and SCALEPACK (Otwinowski and Minor, 1997). X-ray data statistics are summarized in Table I.

Structure determination and refinement

The coordinates of the ERα-LBD–E_2 monomer (PDB entry: 1ERE; Brzozowski *et al.*, 1997), truncated to Tyr526 at the C-terminus and without the ligand, were used as a search model in AMoRe (CCP4, 1994) to solve the structure of the rERβ–RAL complex. Subsequently, the refined coordinates of the rERβ–RAL complex (excluding the ligand and residues after H11) were used in AMoRe to determine the position of the LBD in the GEN complex. A single, clear solution was obtained for both structures using data between 15 and 4 Å and an integration radius of 25–26 Å. Initial electron density maps, calculated after rigid-body refinement in AMoRe, highlighted regions where sequence changes were required and unambiguously indicated the position and orientation of each ligand within the cavity. Both complexes were refined with REFMAC (Murshudov *et al.*, 1997) using all available data with no sigma cut-offs. Bulk solvent contributions, calculated in XPLOR v3.843 (Brünger, 1992), were incorporated in the form of partial structure factors. In both cases, the structures initially were refined against the lower resolution data sets collected at the SRS and LURE prior to the incorporation of the higher resolution terms. For the RAL complex, successive rounds of refinement and manual rebuilding gave a final model with an R_{cryst} of 20.4 and an R_{free} of 26.3 for all data between 25 and 2.25 Å. The final model comprises 1807 protein atoms, 34 ligand atoms, 128 waters and an acetate molecule. Residues prior to T262 at the N-terminus and C481–Y488 (H11–H12 loop) are invisible in the electron density and have not been modelled. The electron density for the H2–H3 loop (S283–S293), H7 (D365–V370) and H12 (A489–A497) is weak but interpretable. H12 has extremely high *B*-values but its inclusion in the model is justified as this results in an appreciable drop in R_{free}. The side chains of seven residues (M295, S333, K353, K425, H428, S463 and H464) display static disorder and have been modelled in two alternative conformations. The final model for the GEN complex, comprising 1834 protein atoms, 20 ligand atoms and 139 waters, has an R_{cryst} of 21.9 and R_{free} of 25.5 for all data between 55 and 1.8 Å. Residues S286–E291 (H2–H3 loop) and T415–D419 (H9–H10 loop) are poorly defined and have not been included in the final model. The side chains of 16 residues (E266, M309, S311, S333, M336, E337, E389, M403, S408, Q450, S463, S469, M473, L477, M478 and N496) and the main chain of two residues (P358–D359) display static disorder and have been modelled in two alternative conformations. All model building was carried out in the molecular graphics package QUANTA (QUANTA98; Molecular Simulations Inc., San Diego, CA). Dictionaries for the ligand molecules were derived from structures built and minimized in QUANTA. Water molecules that made at least one reasonable hydrogen bond to the protein were included as long as their *B*-values remained below 70 $Å^2$. A summary of the refinement and model statistics is given in Table I.

Superpositions of the different ligand complexes were carried out in QUANTA using all equivalent residues up to the end of H11. The remainder of the main chain was excluded due to the large differences in the position of H12. After this global superposition, the overlaps were fine-tuned using the 'match closest residue' option in QUANTA. Cavity volume calculations and surface generation were performed in VOIDOO (Kleywegt and Jones, 1994) using a 0.4 Å primary grid and a probe of radius 1.4 Å. Figures 1, 3, 4 and 5 were produced using BOBSCRIPT (Esnouf, 1997).

Atomic coordinates have been deposited in the Brookhaven Protein Data Bank (accession codes 1QKN and 1QKM for the RAL and GEN complexes, respectively) and are 'on-hold' for 1 year.

Acknowledgements

We would like to thank Julia Walton for help with crystallizations, Stefan Nilsson for discussion and comments on the manuscript and the beamline managers at the ESRF, EMBL-Hamburg, LURE and SRS for technical assistance during data collection. The infrastructure of the Structural Biology Laboratory at York is supported by the BBSRC. We thank the European Union for support of the work carried out at EMBL Hamburg outstation through the HCMP access to large installations project (contract number CHGE-CT93-0040).

References

Adlercreutz,H. and Mazur,W. (1997) Phyto-oestrogens and Western diseases. *Anal. Med.*, **29**, 95–120.

Anstead,G.M., Carlson,K.E. and Katzenellenbogen,J.A. (1997) The estradiol pharmacophore: ligand structure–estrogen receptor binding affinity relationships and a model for the receptor binding site. *Steroids*, **62**, 268–303.

Barkhem,T., Carlsson,B., Nilsson,Y., Enmark,E., Gustafsson, J.-Å. and Nilsson,S. (1998) Differential response of estrogen receptor α and estrogen receptor β to partial estrogen agonists/antagonists. *Mol. Pharmacol.*, **54**, 105–112.

Barton,G.J. (1993) ALSCRIPT: a tool to format multiple sequence alignments. *Protein Eng.*, **6**, 37–40.
Beato,M. and Sanchez-Pacheco,A. (1996) Interaction of steroid hormone receptors with the transcription initiation complex. *Endocr. Rev.*, **17**, 587–609.
Bourguet,W., Ruff,M., Chambon,P., Gronemeyer,H. and Moras,D. (1995) Crystal-structure of the ligand-binding domain of the human nuclear receptor RXR-α. *Nature*, **375**, 377–382.
Brünger,A. (1992) *X-PLOR Version 3.1: A System for X-ray Crystallography and NMR*. Yale University Press, New Haven, CT.
Brzozowski,A.M. *et al*. (1997) Molecular basis of agonism and antagonism in the oestrogen receptor. *Nature*, **389**, 753–758.
Collaborative Computational Project No. 4. (1994) The CCP4 suite: programs for protein crystallography. *Acta Crystallogr. D*, **50**, 760–763.
Danielian,P.S., White,R., Lees,J.A. and Parker,M.G. (1992) Identification of a conserved region required for hormone dependent transcriptional activation by steroid hormone receptors. *EMBO J.*, **11**, 1025–1033.
Darimont,B.D., Wagner,R.L., Apriletti,J.W., Stallcup,M.R., Kushner,P.J., Baxter,J.D., Fletterick,R.J. and Yamamoto,K.R. (1998) Structure and specificity of nuclear receptor–coactivator interactions. *Genes Dev.*, **12**, 3343–3356.
Draper,M.W., Flowers,D.E., Huster,W.J., Neild,J.A., Harper,K.D. and Arnaud,C. (1996) A controlled trial of raloxifene (LY139481) HCl: impact on bone turnover and serum lipid profile in healthy postmenopausal women. *J. Bone Miner. Res.*, **11**, 835–842.
Esnouf,R.M. (1997) An extensively modified version of Molscript that includes greatly enhanced coloring capabilities. *J. Mol. Graph.*, **15**, 132–137.
Fawell,S.E., Lees,J.A., White,R. and Parker,M.G. (1990) Characterisation and colocalization of steroid binding and dimerisation activities in the mouse estrogen receptor. *Cell*, **60**, 953–962.
Feng,W.J., Ribeiro,R.C.J., Wagner,R.L., Nguyen,H., Aprilleti,J.W., Fletterick,R.J., Baxter,J.D., Kushner,P.J. and West,B.L. (1998) Hormone-dependent coactivator binding to a hydrophobic cleft on nuclear receptors. *Science*, **280**, 1747–1749.
Greene,G.L., Nolan,C., Engler,J.P. and Jensen,E.V. (1980) Monoclonal antibodies to the human estrogen receptor. *Proc. Natl Acad. Sci. USA*, **77**, 5115–5119.
Grese,T.A. *et al*. (1997) Molecular determinants of tissue selectivity in estrogen receptor modulators. *Proc. Natl Acad. Sci. USA*, **94**, 14105–14110.
Gustafsson,J.-Å. (1998) Raloxifene: magic bullet for heart and bone? *Nature Med.*, **4**, 152–153.
Jordan,V.C. (1998) Antiestrogenic action of raloxifene and tamoxifen: today and tomorrow. *J. Natl Cancer Inst.*, **90**, 967–971.
Katzenellenbogen,B.S. and Korach,K.S. (1997) A new actor in the estrogen receptor drama—enter ER-β. *Endocrinology*, **138**, 861–862.
Klaholz,B.P., Renaud,J.-P., Mitschler,A., Zusi,C., Chambon,P., Gronemeyer,H. and Moras,D. (1998) Conformational adaptation of agonists to the human nuclear receptor RAR gamma. *Nature Struct. Biol.*, **5**, 199–202.
Kleywegt,G.J. and Jones,T.A. (1994) Detection, delineation, measurement and display of cavities in macromolecular structures. *Acta Crystallogr. D*, **50**, 178–185.
Korach,K. (1994) Insights from the study of animals lacking functional estrogen receptor. *Science*, **266**, 1524–1527.
Krege,J.H. *et al*. (1998) Generation and reproductive phenotypes of mice lacking estrogen receptor β. *Proc. Natl Acad. Sci. USA*, **95**, 15677–15682.
Kuiper,G.G.J.M., Enmark,E., Pelto-Huikko,M., Nilsson,S. and Gustafsson, J.-Å. (1996) Cloning of a novel estrogen receptor expressed in rat prostate and ovary. *Proc. Natl Acad. Sci. USA*, **93**, 5925–5930.
Kuiper,G.G.J.M., Carlsson,B., Grandien,J., Enmark,E., Häggblad,J., Nilsson,S. and Gustafsson, J.-Å. (1997) Comparison of the ligand binding specificity and transcript tissue distribution of the estrogen receptors α and β. *Endocrinology*, **138**, 863–870.
Laskowski,R.A., MacArthur,M.W., Moss,D.S. and Thornton,J.M. (1993) PROCHECK—a program to check the stereochemical quality of protein structures. *J. Appl. Crystallogr.*, **26**, 283–291.
MacGregor,J.I. and Jordan,V.C. (1998) Basic guide to the mechanisms of antiestrogen action. *Pharmacol. Rev.*, **50**, 151–196.
McInerney,E.M., Weis,K.E., Sun,J., Mosselman,S. and Katzenellenbogen, B.S. (1998) Transcription activation by the human estrogen receptor subtype β (ERβ) studied with ERβ and ERα receptor chimeras. *Endocrinology*, **139**, 4513–4522.
Moras,D. and Gronemeyer,H. (1998) The nuclear receptor ligand-binding domain: structure and function. *Curr. Opin. Cell Biol.*, **10**, 384–391.
Murshudov,G.N., Vagin,A.A. and Dodson,E.J. (1997) Refinement of macromolecular structures by the maximum-likelihood method. *Acta Crystallogr. D*, **53**, 240–255.
Nolte,R.T. *et al*. (1998) Ligand-binding and co-activator assembly of the peroxisome proliferator-activated receptor-γ. *Nature*, **395**, 137–143.
Ogawa,S., Inoue,S., Watanabe,T., Hiroi,H., Orimo,A., Hosoi,T., Ouchi,Y. and Muramatsu,M. (1998) The complete primary structure of human estrogen receptor β (hERβ) and its heterodimerisation with ERα *in vivo* and *in vitro*. *Biochem. Biophys. Res. Commun.*, **243**, 122–126.
Otwinowski,Z. and Minor,W. (1997) Processing X-ray diffraction data collected in oscillation mode. *Methods Enzymol.*, **276**, 307–326.
Paech,K., Webb,P., Kuiper,G.G.J.M., Nilsson,S., Gustafsson,J.-Å., Kushner,P.J. and Scanlan,T.S. (1997) Differential ligand activation of estrogen receptors ERα and ERβ at AP1 sites. *Science*, **277**, 1508–1510.
Renaud,J.P., Rochel,N., Ruff,M., Vivat,V., Chambon,P., Gronemeyer,H. and Moras,D. (1995) Crystal structure of the RAR-γ ligand-binding domain bound to all-*trans* retinoic acid. *Nature*, **378**, 681–689.
Shiau,A.K., Barstad,D., Loria,P.M., Cheng,L., Kushner,P.J., Agard,D.A. and Greene,G.L. (1998) The structural basis of estrogen receptor/coactivator recognition and the antagonism of this interaction by tamoxifen. *Cell*, **95**, 927–937.
Stickle,D.F., Presta,L.G., Dill,K.A. and Rose,G.D. (1992) Hydrogen bonding in globular proteins. *J. Mol. Biol.*, **226**, 1143–1159.
Tanenbaum,D.M., Wang,Y., Williams,S.P. and Sigler,P.B. (1998) Crystallographic comparison of the estrogen and progesterone receptor's ligand binding domains. *Proc. Natl Acad. Sci. USA*, **95**, 5998–6003.
Torchia,J., Glass,C.K. and Rosenfeld,M.G. (1998) Co-activators and co-repressors in the integration of transcriptional responses. *Curr. Opin. Cell Biol.*, **10**, 373–383.
Tsai,M.-J. and O'Malley,B.W. (1994) Molecular mechanisms of action of steroid/thyroid receptor superfamily members. *Annu. Rev. Biochem.*, **63**, 451–486.
Wagner,R.L., Apriletti,J.W., McGrath,M.E., West,B.L., Baxter,J.D. and Fletterick,R.J. (1995) A structural role for hormone in the thyroid hormone receptor. *Nature*, **378**, 690–697.
Wurtz,J.-M., Bourguet,W., Renaud,J.-P., Vivat,V., Chambon,P., Moras,D. and Gronemeyer,H. (1996) A canonical structure for the ligand-binding domain of nuclear receptors. *Nature Struct. Biol.*, **3**, 87–94.

Received May 27, 1999; revised and accepted July 5, 1999